

MDEV versus ADEV

W.J. Riley
Hamilton Technical Services
Beaufort, SC 29907 USA
Rev A. August 23, 2020

• Introduction

This document compares the properties and usage of the normal and Modified Allan deviations as stability measures for a frequency source. These statistics are well-known alternatives to the standard deviation for devices having divergent power law noise¹, but their characteristics and applicability are not always well understood.

As a first example, the Figure 1 composite stability plot shows the normal and modified Allan deviations (ADEV and MDEV) for 10,000 points of simulated W PM noise having a stability of $\sigma_y(\tau_0=1s) = 1 \times 10^{-11}$. Their log-log slopes are -1.0 and -1.5 respectively².

A good starting point for studying the relationship between the Allan and Modified Allan variances is Section A.6 on Page TN-9 of Reference [1]. In particular, the two excerpts from that information copied below as Figures 14 and 15 allow easy comparison and conversion between AVAR and MVAR. Mod $\sigma_y(\tau)$ is always smaller than $\sigma_y(\tau)$, particularly for white and flicker PM noise. MDEV thus provides effective filtration for those noises, an advantage for some measurements but which can also underestimate source instability.

Roughly speaking, MDEV is similar to ADEV for white, flicker and random walk FM noise, and decreases more rapidly versus averaging factor for flicker and white PM noise. MDEV is equal to ADEV at the basic sampling interval, τ_0 , and is always smaller than ADEV for averaging factors greater than 1. It is much less widely used than ADEV, mainly to distinguish between those PM noise types, and indirectly as the basis of the time deviation, TDEV. Most stability specifications are in terms of ADEV, which is somewhat faster to calculate and has somewhat higher confidence. MDEV usage is highest in the timing and telecom fields.

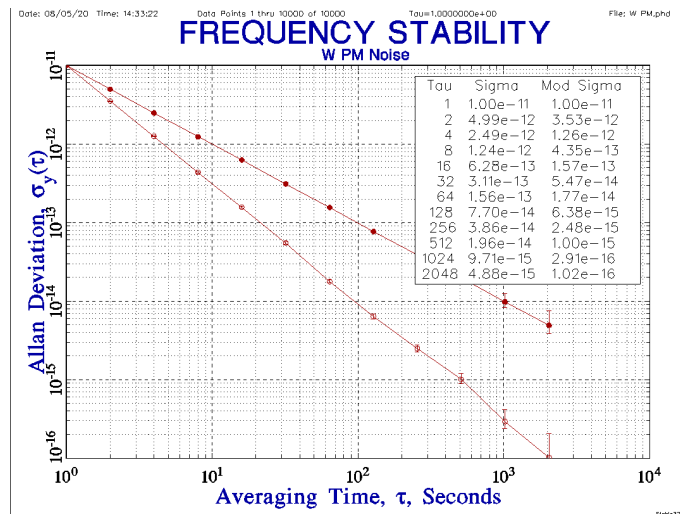


Figure 1. ADEV and MDEV for W PM Noise

The ratio $R(n) = \text{MVAR}/\text{AVAR}$ as a function of averaging factor $n = \tau/\tau_0$ for W PM noise = $1/n$ (see Fig. 15), as seen above by their x10 deviation ratio at $\tau=10^2$ s. Notice also the wider MDEV error bars.

¹ The noise of frequency sources is commonly modeled by five power law spectral density terms, $h_\alpha f^\alpha$, where the Fourier frequency exponent, α , ranges from -2 to +2 corresponding to the random walk FM, flicker FM, white FM, flicker PM and white PM noise types, where the $\alpha=-2$ and -1 terms display non-convergent standard deviations (see Sections 3.2 and 5.2.1 of Reference [14]). See [Appendix 1](#).

² This figure and many of the other stability plots in this paper were generated by the Stable32 program for frequency stability analysis which is freely available from the [IEEE UFFC](#).

- **ADEV**

The Allan deviation, $\sigma_y(\tau)$ or ADEV, introduced in 1966 in Reference [7], is the most commonly-used time domain measure for frequency stability, and, as such, we assume that it is familiar to the reader. To briefly review, it was developed as an alternative to the standard deviation, σ , because latter does not converge to a consistent value for the flicker and even more divergent FM noise processes often associated with frequency sources. ADEV uses 1st differences of frequency instead of the frequency average. The subscript y in the symbol for the ADEV denotes dimensionless fractional frequency stability, $y(t) = (f(t) - f_o) / f_o$, and its τ dependence indicates that it is a function of the averaging time associated with the analysis. Phase fluctuations, in units of seconds, are denoted by $x(t)$. Frequency is the rate of change of phase, $y(t) = dx(t) / dt$. Please see [11], [14], [19], [20], [25], [35], or other similar references for definitions and basic information about frequency stability analysis and power-law noise models.

Keeping in mind the distinction between a statistic and its estimator, one can calculate the Allan deviation via several methods, e.g., its original naive estimator, the preferable fully-overlapping ADEV formula, or more elaborately by other, possibly biased, estimators such as the Total or Th  l deviations. The latter methods, although involving more complicated formulae, have the advantage of providing higher confidence and results at longer averaging factors.

- **Non-Overlapping Allan Variance**

The Allan, or 2-sample variance, AVAR, is the most common time domain measure of frequency stability. Its non-overlapping version is defined as:

$$\sigma_y^2(\tau) = \frac{1}{2(M-1)} \sum_{i=1}^{M-1} [y_{i+1} - y_i]^2, \quad \text{This original estimator of the 2-sample or Allan variance closely resembles its definition using the 1st differences of the fractional frequency variations.} \quad (1)$$

where y_i is the i^{th} of M fractional frequency values averaged over the measurement interval τ .

In terms of phase data, the Allan variance may be calculated as:

$$\sigma_y^2(\tau) = \frac{1}{2(N-2)\tau^2} \sum_{i=1}^{N-2} [x_{i+2} - 2x_{i+1} + x_i]^2, \quad \text{This is the same AVAR estimator as Eq. (1) using the 2nd differences of the phase variations.} \quad (2)$$

where x_i is the i^{th} of the N = M+1 phase values spaced by the measurement interval τ .

The result is usually expressed as its square root, $\sigma_y(\tau)$, the Allan deviation, ADEV. The Allan variance has the same expected value as the ordinary variance for white FM noise, but has the advantage, for more divergent noise types such as flicker FM noise, of converging to a value that is not dependent on the number of data points. The confidence interval of an Allan deviation estimate is also dependent on the noise type, but is often simply estimated as $\pm\sigma_y(\tau)/\sqrt{N}$, perhaps including a correction factor for the noise type (see Section 5 of [19] or Section 5.3.1 of [14])³.

- **Overlapping Allan Variance**

The overlapping Allan variance is a version of the Allan variance, $\sigma_y^2(\tau)$, AVAR, that makes maximum use of a data set by forming all possible fully overlapping samples at each averaging time τ . It can be

³ Even approximate error bars are better than none. Most ADEV specifications use the nominal, not upper error bar, value.

estimated from a set of M frequency measurements for averaging time $\tau = m\tau_0$, where m is the averaging factor and τ_0 is the basic measurement interval, by the expression:

$$\sigma_y^2(\tau) = \frac{1}{2m^2(M-2m+1)} \sum_{j=1}^{M-2m+1} \left\{ \sum_{i=j}^{j+m-1} [y_{i+m} - y_i] \right\}^2 \quad \text{This fully-overlapping estimator of the 2-sample or Allan variance using the 1st differences of the fractional frequency variations has higher confidence than that of Eq. (1).} \quad (3)$$

In terms of phase data, the overlapping Allan variance can be estimated from a set of N = M+1 time measurements as:

$$\sigma_y^2(\tau) = \frac{1}{2(N-2m)\tau^2} \sum_{i=1}^{N-2m} [x_{i+2m} - 2x_{i+m} + x_i]^2, \quad \text{This is the same AVAR estimator as Eq. (3) using the 2nd differences of the phase variations.} \quad (4)$$

The result is usually expressed as the square root, $\sigma_y(\tau)$, the Allan deviation, ADEV. The confidence interval of an overlapping Allan deviation estimate is better than that of a non-overlapping Allan variance estimation because, even though the additional overlapping differences are not all statistically independent, they nevertheless increase the number of degrees of freedom and thus improve the confidence in the estimation. Analytical methods are available for calculating the number of degrees of freedom for an overlapping Allan variance estimation, and for using that to establish single or double-sided confidence intervals for the estimate with a certain confidence factor, based on Chi-squared statistics (see Section 5 of [19] or Section 5.3.2 of [14]).

Sample variances are distributed according to the expression:

$$\chi^2 = \frac{df \cdot s^2}{\sigma^2} \quad (5)$$

where χ^2 is the Chi-square, s^2 is the sample variance, σ^2 is the true variance, and df is the # of degrees of freedom (not necessarily an integer). The df is determined by the # of data points and the noise type.

Herein, ADEV generally refers to any of these Allan deviation estimators, but most specifically to the fully-overlapping method, preferably using phase data.

• MDEV

The Modified Allan variance, Mod $\sigma_y^2(\tau)$ or MVAR, introduced in 1981 in Reference [8], is an alternative to the normal Allan variance that includes phase averaging in its estimation process. The phase averaging varies the analysis bandwidth, dividing it by the averaging factor, n, by averaging n adjacent phase samples. MVAR equals AVAR at unity averaging factor and is smaller at all larger ones. The addition filtering makes MDEV independent of the measuring system bandwidth under most conditions⁴.

The MDEV is used mainly to distinguish between white and flicker PM noise, as shown in Figures 1 and 2-3, and serves as the basis of the time deviation, TDEV. As such, MDEV is particularly useful for analyzing frequency sources like crystal oscillators and active H masers. It is slightly more

⁴ The relationships between phase noise type and level, ADEV and MDEV values, measurement tau (τ_0), averaging factor and system bandwidth can be explored with the Stable32 Domain function. For example, one can use constant values of PSD Type, Carrier Freq, SB Freq, Carrier Freq and W or F PM noise, and observe the variation in ADEV or MDEV versus analysis tau ($\tau=\tau_0 \cdot AF$) and/or BW factor. One will notice that, for W PM, ADEV varies with AF for the same analysis tau and other parameters while MDEV does not, and that MDEV is independent of the system upper cutoff frequency, f_h .

computationally intensive and has somewhat less confidence than ADEV. Note that the ADEV white and flicker F PM noise slopes are both about -1.0 while they are -1.5 and -1.0 respectively for MDEV. MDEV can also be used to suppress instrumental white PM noise in an FM noise analysis (see Fig. 6).

The modified Allan variance, $\text{Mod } \sigma_y^2(\tau)$, MVAR, is estimated from a set of M frequency measurements for averaging time $\tau = m\tau_0$, where m is the averaging factor and τ_0 is the basic measurement interval, by the expression:

$$\text{Mod } \sigma_y^2(\tau) = \frac{1}{2m^4(M-3m+2)} \sum_{j=1}^{M-3m+2} \left\{ \sum_{i=j}^{j+m-1} \left(\sum_{k=i}^{i+m-1} [y_{k+m} - y_k] \right) \right\}^2. \quad (6)$$

MDEV is proportional to the 1st difference of the fractional frequency variations averaged over m adjacent samples.

Because of the triple-nested nature of this expression, it is better to perform an MVAR calculation with phase data, especially for a run over multiple averaging factors.

In terms of phase data, the modified Allan variance is estimated from a set of N = M+1 time measurements as:

$$\text{Mod } \sigma_y^2(\tau) = \frac{1}{2m^2\tau^2(N-3m+1)} \sum_{j=1}^{N-3m+1} \left\{ \sum_{i=j}^{j+m-1} [x_{i+2m} - 2x_{i+m} + x_i] \right\}^2. \quad (7)$$

MDEV is proportional to the 2nd difference of the phase variations averaged over tau.

There is a recursive algorithm for this estimator that speeds up its computation, see [13]. The result is usually expressed as the square root, MDEV or $\text{Mod } \sigma_y(\tau)$, the modified Allan deviation. The modified Allan variance is the same as the normal Allan variance for m = 1. It includes an additional phase averaging operation, the m-point moving average i summations in Eqs. (6) and (7), and has the advantage of being able to distinguish between white and flicker PM noise. The edf and confidence interval of a modified Allan deviation determination are also dependent on the noise type [18], and can also set simply as $\pm \text{Mod } \sigma_y(t)/\sqrt{N}$, including a noise correction factor, or by Chi-squared statistics.

Figures 2-5 show examples of MDEV and ADEV plots for white and flicker PM noise.

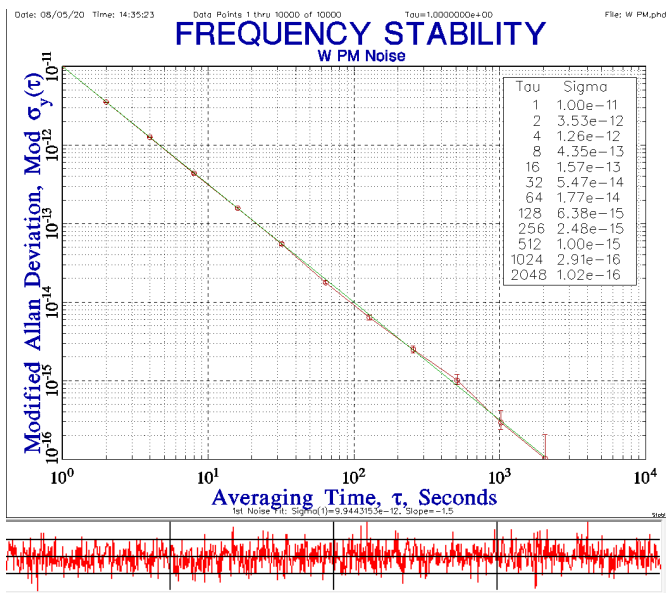


Figure 2. MDEV for W PM Noise
Log-Log Slope=-1.5

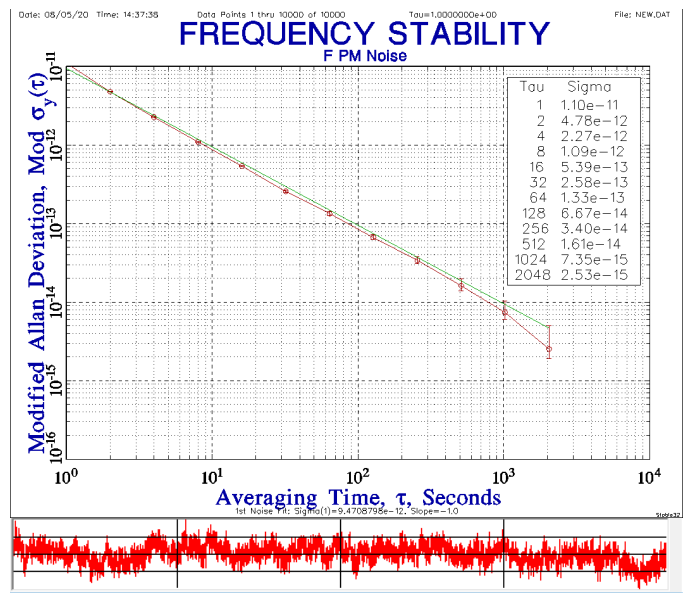


Figure 3. MDEV for F PM Noise
Log-Log Slope=-1.0

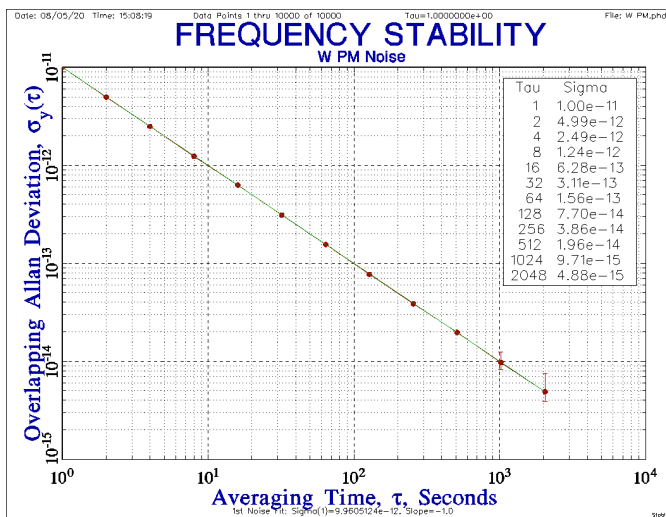


Figure 4 ADEV for W PM Noise
Log-Log Slope=-1.0

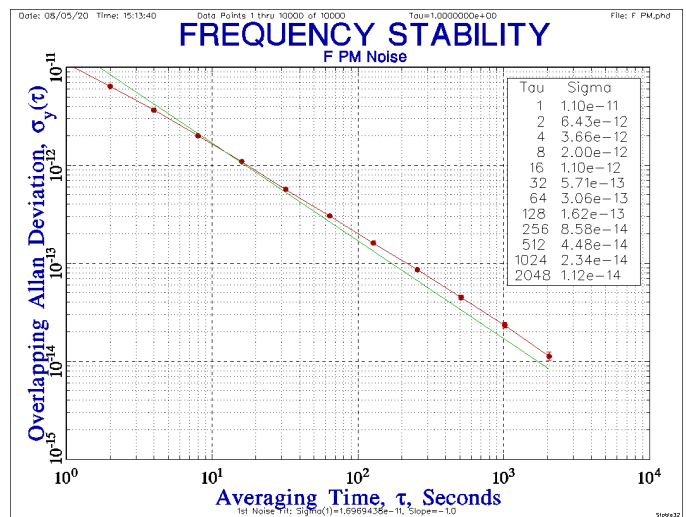


Figure 5 ADEV for F PM Noise
Log-Log Slope=-1.0

Quoting from Reference [9]:

AVAR may be shown to be an optimum estimator for variations in frequency for atomic clocks. TVAR may be shown to be an optimum estimator for variations in time or phase, such as for measurement systems, telecommunication networks, etc. MVAR allows one to observe both clock and measurement instabilities in a near optimum way and it removes the ambiguity problem existing for AVAR for power-law spectral density values where $\alpha \geq 1$.

ADEV should be used in preference to MVAR for most purposes, especially for $\alpha < +1$, but it can be a valuable analytical tool for distinguishing white and flicker PM noise ($\alpha = -2$ and -1), and, along with TDEV, for analyzing the stability of time sources and distribution systems [5].

As an example of the ability of MDEV to suppress white PM noise contamination, consider the ADEV and MDEV stability plots of Figure 6 for the combination of W FM noise at a simulated level of $1e-11$ at 1s (say from a rubidium frequency standard under test) plus W PM noise at a higher level of $5e-11$ at 1s (say from the noise floor of a clock measurement system). The objective is to determine the level of the RFS W FM noise (shown by the green line). The usual way would be to fit a W FM line to the ADEV results where the slope is $\tau^{-1/2}$, say at 1000s. This gives the correct result. But notice that the MDEV plot reaches the W FM slope much faster, say at 50s, and the R(n) ratio can then be used to obtain an ADEV estimate of $1e-12/\sqrt{0.5}=1.4e-12$, in good agreement with the direct ADEV value but 20x faster.

• **TDEV**

The Modified Allan variance, $\text{Mod } \sigma_y^2(\tau)$ or MVAR is also the basis of the Time variance and its deviation, TDEV. TVAR is a measure of time stability and is defined as [15], [16], [17]:

$$\sigma_x^2(\tau) = (\tau^2 / 3) \cdot \text{Mod } \sigma_y^2(\tau) . \tag{8}$$

TVAR is equal to the standard variance of the time deviations for white PM noise. Its square root, TDEV is MDEV with a log-log slope transposed by +1 and scaled by $\sqrt{3}$. Because of that simple relationship, one can show loci of constant TDEV on an MDEV plot as shown in Figure 7.

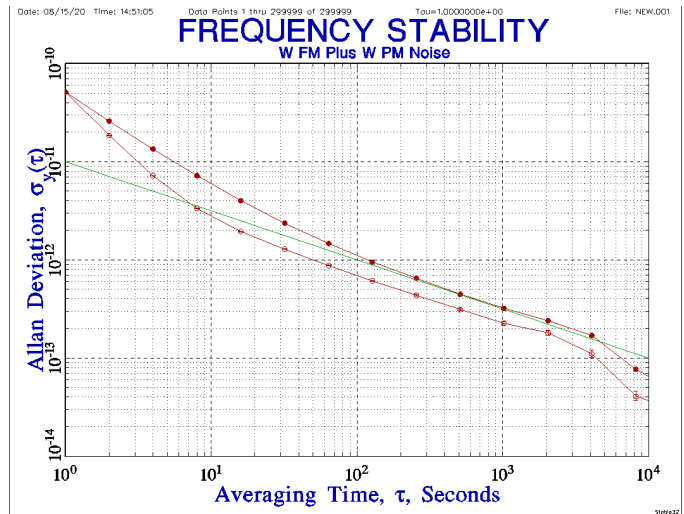


Figure 6. ADEV and MDEV Stability Plots for $\sigma_y(\tau)=1 \times 10^{-11} \tau^{-1/2}$ W FM RFS Noise Contaminated with $\sigma_y(\tau)=5 \times 10^{-11} \tau^{-1}$ W PM Instrumental Noise

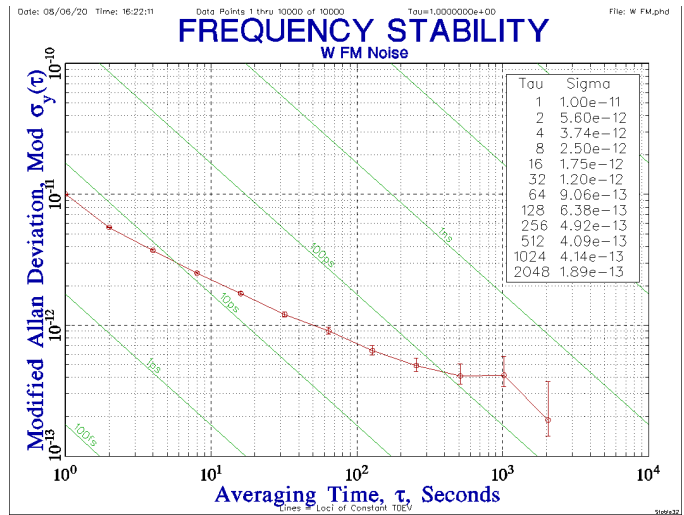


Figure 7. MDEV Plot with TDEV Loci

TDEV is commonly used to characterize the time error of a time source (clock), or telecommunications or distribution system [12], [33]. It makes sense to specify the requirements of a timing system in terms of TDEV, especially one for which there is a critical time interval such as a GPS satellite clock with 1-day updates⁵.

The time error of a clock, ΔT , is the sum of the effects of initial time synchronization offset, T_0 , initial frequency syntonization offset, $\Delta f/f$, subsequent frequency drift caused by internal aging and environmental sensitivity, D , and stochastic time variations, σ_x .

⁵ What ADEV is required for a 1-day TDEV = 1 ns resulting from the W FM noise of an atomic clock? The corresponding MDEV is $\text{sqrt}(3e-18/86,400^2) = 2.00e-14$ at 1-day. $R(n)$ (see Fig. 14) for W FM noise is 0.5, so ADEV is $2.00e-13/\sqrt{0.5} = 2.84e-14$ at 1-day and the required clock stability is $\sigma_y(\tau) \leq 8.34e-12 \tau^{-1/2}$. A Stable32 simulation will confirm this.

$$\Delta T = T_0 + (\Delta f / f) \cdot t + 1/2 \cdot D \cdot t^2 + \sigma_x(t). \tag{9}$$

The deterministic time error due to frequency offset integrates linearly and that caused by frequency drift integrates quadratically. The effect of environmental sensitivities can be quite complex depending on when and how they occur. TDEV describes the stochastic time error. The overall time error thus depends on how these various mechanisms combine. The resulting error budget is more complex for a moderate-performance source in a tactical environment than for a high-stability device under benign conditions. The overall system may have means for initial synchronization and periodic resynchronization, and those provisions may have their own error considerations. In the long run, clock reliability may be the most important factor⁶. A multiple-clock ensemble can improve both reliability and performance⁷.

• Sigma-Tau Plots

Sigma-Tau plots for ADEV, MDEV and TDEV show the different white and flicker PM noise slopes for the former two, and the +1 slope translation for TDEV. The generic plots of Figures 8-10 show the general trend of increasing slope versus longer averaging time, and the dominance of PM noise in the short term, FM noise in the medium term, and frequency drift at long term.

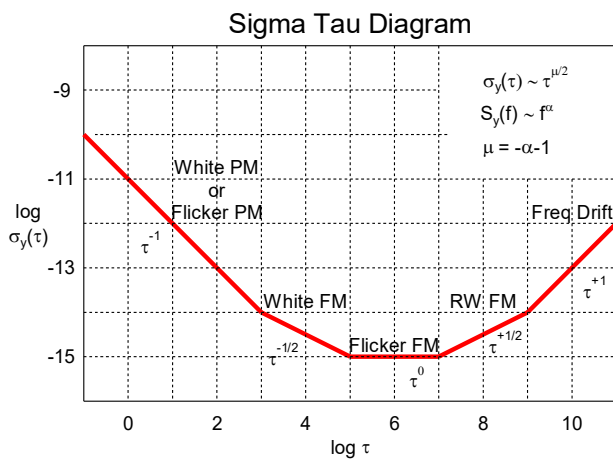


Figure 8. ADEV Sigma-Tau Diagram

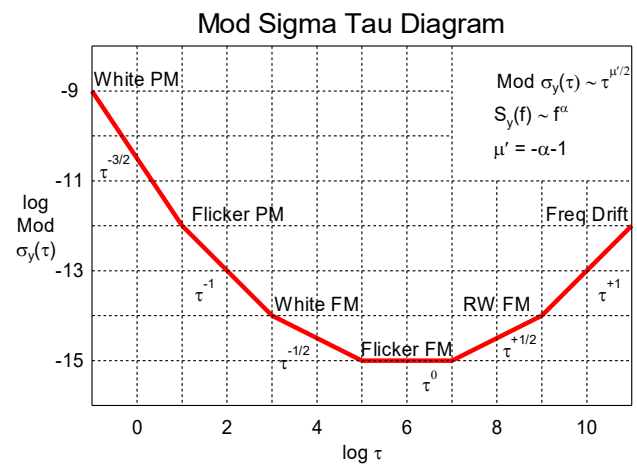


Figure 9. MDEV Sigma-Tau Diagram

⁶ A clock must obviously run continuously, and that is sometimes the distinction between a clock and a frequency standard.

⁷ The stability of a clock ensemble can exceed that of its individual members.

Sigma-Tau diagrams, log-log plots of ADEV, MDEV, or TDEV versus averaging time, tau, are the most common way to show time domain frequency stability. In most cases, an ADEV plot is preferred. For crystal oscillators, active H-masers and other devices where PM noise is of particular interest, a MDEV plot can distinguish between white and flicker PM noise. Passive atomic clocks are usually dominated by white and flicker FM noise. Most frequency sources show frequency drift at long term. A TDEV plot is often the best way to show the time stability of a timing source or time distribution system.

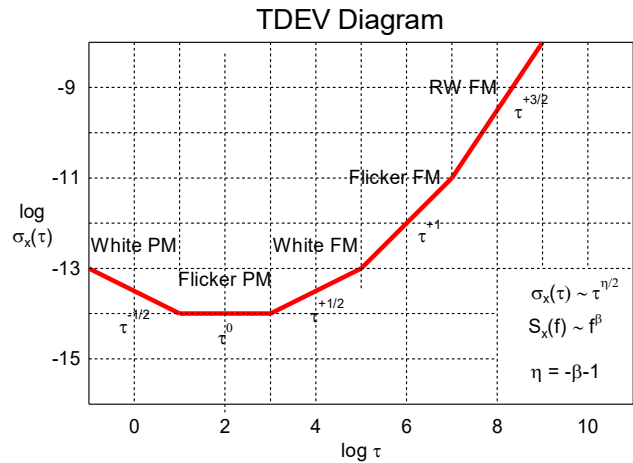
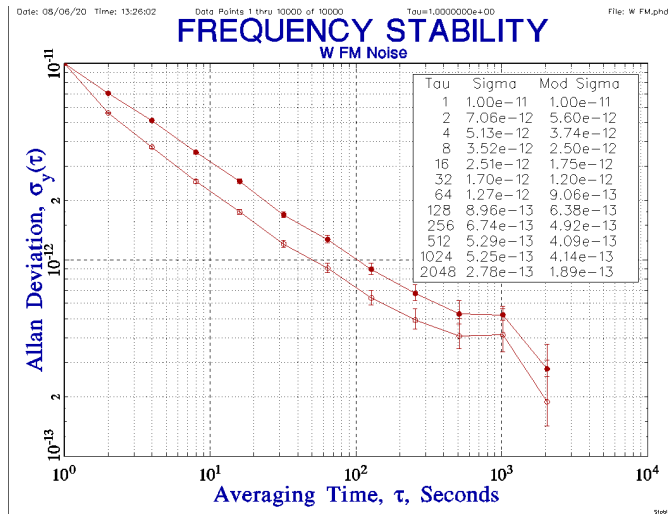


Figure 10. TDEV Sigma-Tau Diagram

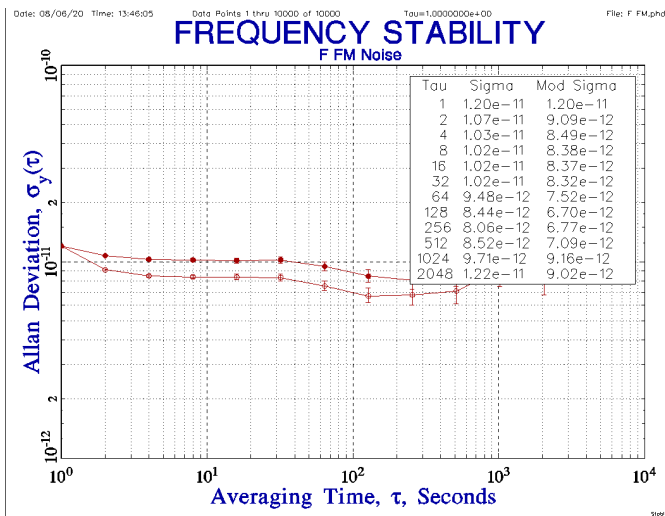
Real data will seldom have all slopes and may not show them, so clearly so it will not always be possible to identify the noise type easily, but it is often effective to fit regions of a sigma-tau plot to a specific power law slope. Other non-graphical methods exist for determining the dominant power-law noise type from a set of phase or frequency data [31].

• **ADEV and MDEV Plots**

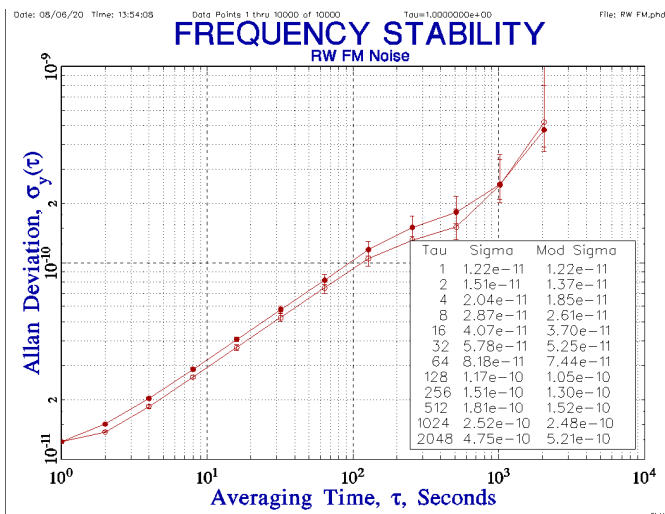
A Set of dual ADEV and MDEV plots for white, flicker and random walk FM noise are shown in Figure 11, along with their expected and actual R(n) differences at an averaging factor of n=128.



ADEV @ AF=128: 8.9601e-13
MDEV @ AF=128: 6.3769e-13
W FM $\alpha=0$ expected $R(128) = 0.500$
Actual $R(128) = (6.3769/8.9601)^2 = 0.506$



ADEV @ AF=8.4431e-12
MDEV @ AF=6.7010e-12
F FM $\alpha=-1$ expected $R(128) = 0.575$
Actual $R(128) = (6.7010/8.4431)^2 = 0.630$



ADEV @ AF=128: 1.1686e-10
MDEV @ AF=128: 1.0489e-10
RW FM $\alpha=-20$ expected $R(128) = 0.825$
Actual $R(128) = (1.0489/1.1686)^2 = 0.806$

Figure 11. Dual ADEV/MDEV Plots for White, Flicker, and Random Walk FM Noise

The actual $R(n)$ values are in good agreement with those expected.

Figure 12 shows a set of ADEV and MDEV plots for various power law noise types from Reference [6] (plus Hadamard variance, HDEV, plots that can be ignored for our present purposes, although it is worth noting that there is also a modified version of it also).

Figure 13 also shows a set of ADEV, MDEV, and TDEV plots for various power law noise types, plotted together.

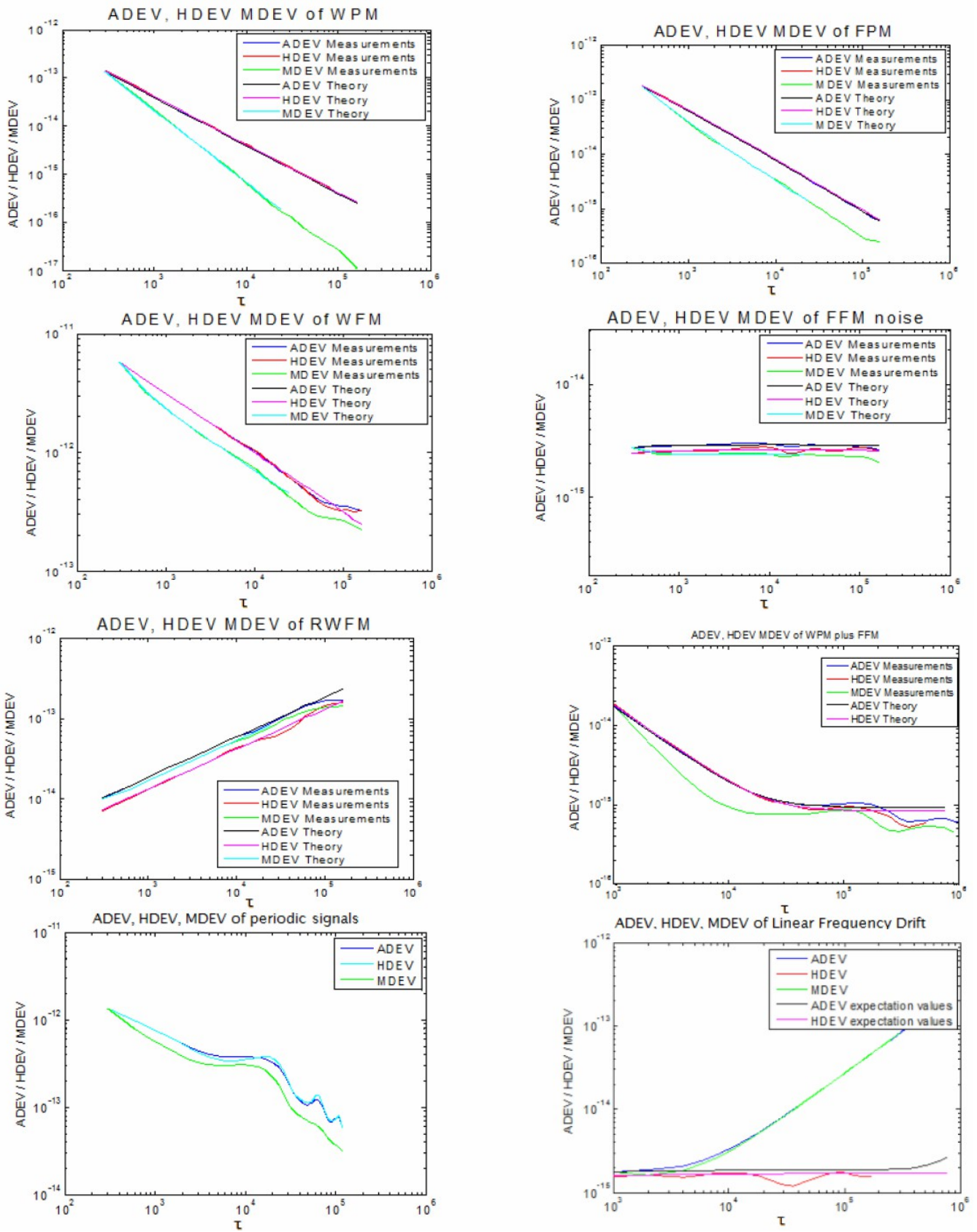


Figure 12. ADEV and MDEV Plots for Various Noise Types (From [6])

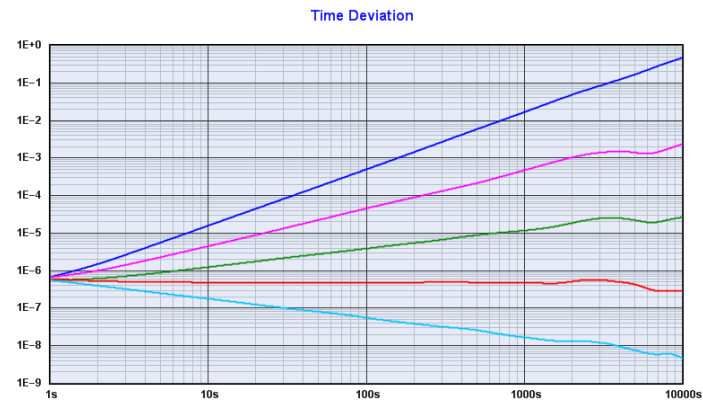
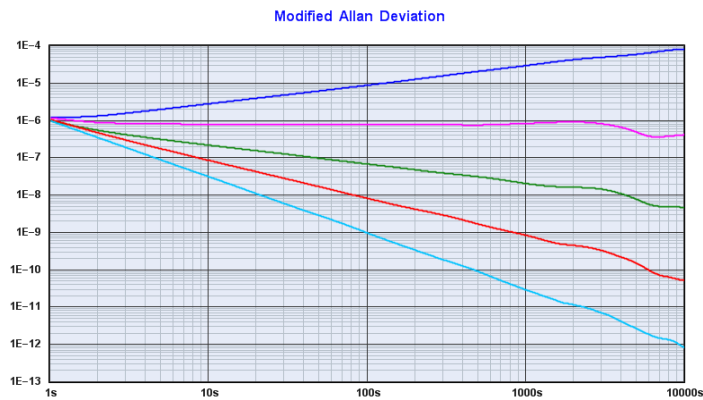
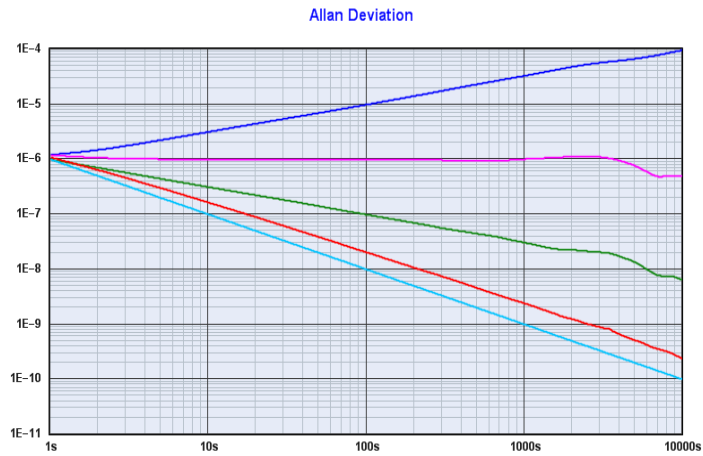


Figure 13. Allan, Modified Allan, and Time Deviation Stability Plots for 10^5 Points of Simulated RW FM (Blue lines, $\alpha=-2$), F FM (Magenta lines, $\alpha=-1$), W FM (Green lines, $\alpha=0$), F PM (Red lines, $\alpha=1$), and W PM (Cyan lines, $\alpha=2$) Power Law Noise. Noise generated by [Stable32](#), plots produced by [TimeLab](#). From: [leapsecond.com](#).

In Figure 12, the linear ADEV (blue) and MDEV (green) plots for the pure power law noise types from W PM, F PM, W FM, F FM, and RW FM show a progression of variations from the MDEV lines having a significantly steeper negative slope to lines where the two statistics essentially overlap. Most of all, these plots show the ability of the MDEV slope to distinguish between white and flicker PM noise. They also show that the MDEV values lie below ($\approx \times 0.707$) the corresponding ADEV values for white FM noise, somewhat below ($\approx \times 0.822$) for flicker FM noise and slightly below ($\approx \times 0.908$) for random walk FM noise. ADEV and MDEV are both equally sensitive to linear frequency drift.

- **The R(n) Bias Function**

The R(n) bias function is the ratio of the Modified Allan variance, MVAR, to the Allan Variance, AVAR (these variances are, of course, equal to the squares of their corresponding deviations). It is a function of the averaging factor, $n=\tau/\tau_0$, and the power law noise type.

For flicker and white PM noise ($a \geq 1$), $\text{Mod } \sigma_y(\tau)$ depends on t_0 , e.g., $\text{Mod } \sigma_y(10n, \tau_0) = \sqrt{10} \cdot \text{Mod } \sigma_y(n, 10\tau_0)$. The effect of white and flicker PM noise on a measurement of the average frequency can be eliminated by making t_0 small and/or n large. See Rutman & Walls 1991 [2].

The following Figures 14 and 15 showing the R(n) bias function are from NIST Technical Note 1337, [*Characterization of Clocks and Oscillators*](#), February 1990 [1]. Section A.6 of that document contains much useful information about the relationship between ADEV and MDEV.

Table 2. Ratio of $\text{mod } \sigma_y^2(\tau)$ to $\sigma_y^2(\tau)$ versus n for common power-law noise types $S_x(f) = h_a f^\alpha$. n is the number of time or phase samples averaged to obtain $\text{mod } \sigma_y^2(\tau = n\tau_0)$ where τ_0 is the minimum sample time. ω_h is 2π times the measurement bandwidth f_b .

$$R(n) = \frac{\text{mod } \sigma_y^2(\tau)}{\sigma_y^2(\tau)} \quad \text{vs. } n \quad \tau = n\tau_0$$

n	$\alpha = -2$	$\alpha = -1$	$\alpha = 0$	$\omega_h \tau_0 = 3$	$\omega_h \tau_0 = 10$	$\omega_h \tau_0 = 100$	$\omega_h \tau_0 = 10^4$	$\alpha = +2$
1	1.000	1.000	1.000	1.000	1.000	1.000	1.000	1.000
2	0.859	0.738	0.616	0.568	0.543	0.525	0.504	0.500
3	0.840	0.701	0.551	0.481	0.418	0.384	0.355	0.330
4	0.831	0.681	0.530	0.405	0.359	0.317	0.284	0.250
5	0.830	0.684	0.517	0.386	0.324	0.279	0.241	0.200
6	0.828	0.681	0.514	0.349	0.301	0.251	0.214	0.167
7	0.827	0.679	0.507	0.343	0.283	0.235	0.195	0.143
8	0.827	0.678	0.506	0.319	0.271	0.219	0.180	0.125
10	0.826	0.677	0.504	0.299	0.253	0.203	0.160	0.100
14	0.826	0.675	0.502	0.274	0.230	0.179	0.137	0.0714
20	0.825	0.675	0.501	0.253	0.210	0.163	0.119	0.0500
30	0.825	0.675	0.500	0.233	0.194	0.148	0.106	0.0333
50	0.825	0.675	0.500	0.210	0.176	0.134	0.0938	0.0200
100	0.825	0.675	0.500	0.186	0.159	0.121	0.0837	0.0100
Limit	0.825	0.675	0.500	$\frac{3.37}{1.04 + 3 \ln \omega_h \tau}$				1/n

Figure 14. R(n) Table for Various Noise Types (From [1])

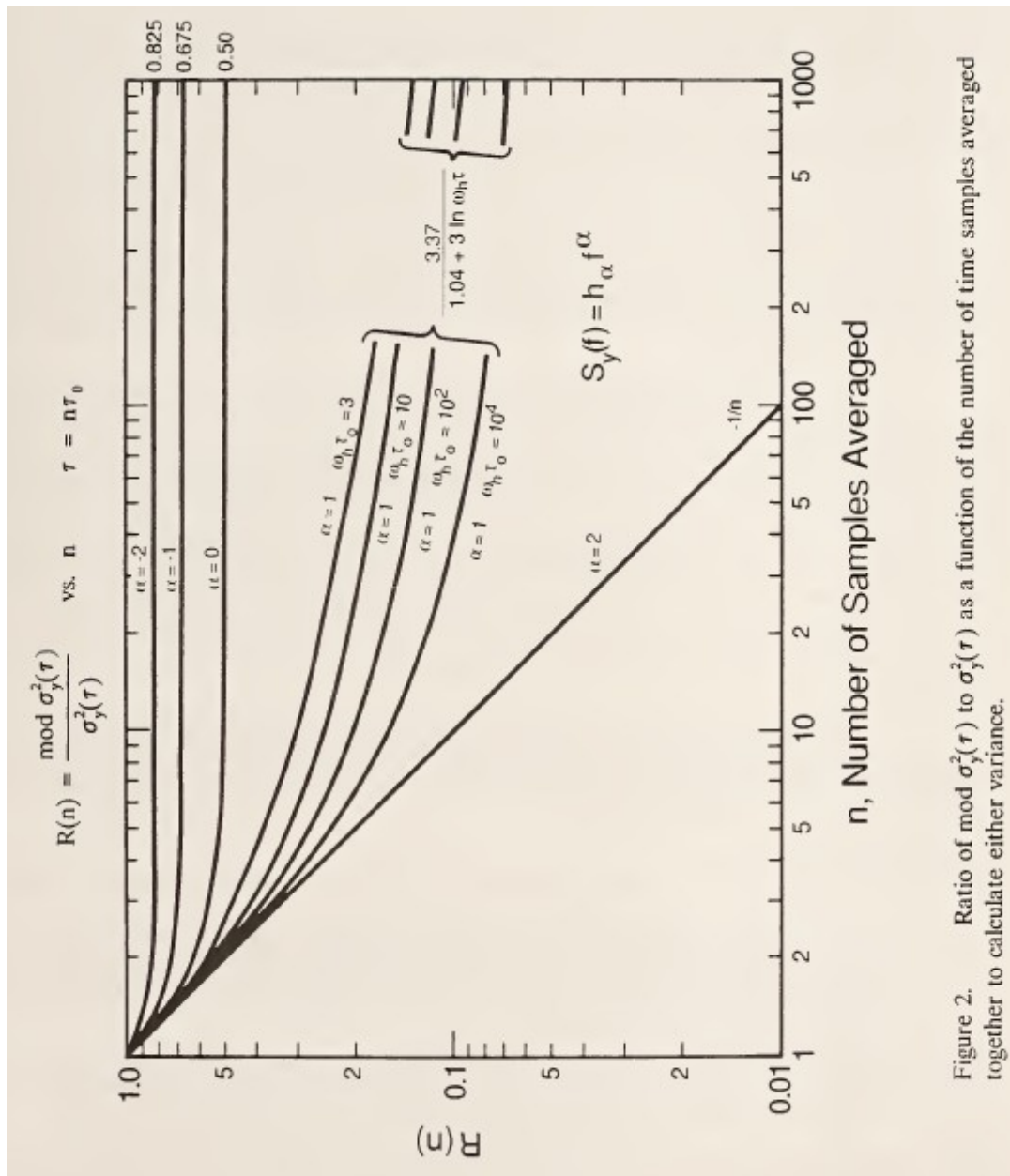


Figure 2. Ratio of $\text{mod } \sigma_y^2(\tau)$ to $\sigma_y^2(\tau)$ as a function of the number of time samples averaged together to calculate either variance.

Figure 15. $R(n)$ Plot for Various Noise Types (From [1])

Analytical expressions for $R(n)$ for the various power law noise types are shown in the table of Figure 16 from Reference [4]. The values for RW FM ($\alpha=-2$), F FM ($\alpha=-1$), and W FM ($\alpha=0$) are 0.825, 0.675 and 0.500 respectively for averaging factors, n , greater than about 10. $R(n)$ is equal to $1/n$ for white PM ($\alpha=2$) noise. The $R(n)$ expression for flicker PM noise ($\alpha=1$) is more complex and depends on the system bandwidth. Note that the corrected values for F FM ($\alpha=-1$) above are slightly different than in the table below. For F PM ($\alpha=1$) the $R(\infty)$ limit (see [10]) is $1.124/\ln(\omega_h\tau)$. Note also that the symbols m and af or AF are also commonly used for the averaging factor, n . Note also that $R(\infty)$ is independent of the system bandwidth, $\omega_h=2\pi f_h$, for W PM ($\alpha=2$).

For F PM ($\alpha=-1$) noise simulated in Stable32 [32], where the equivalent bandwidth is equal to the Nyquist frequency $(2\cdot\tau_0)^{-1}$, $\omega\tau_0=\pi$, and the top R(n) line applies, we would expect a value of $R(128) \approx 0.178$ to apply⁸. If we compare Figures 3 and 5 at AF=128, we find $MVAR/AVAR = (6.67e-14/1.62e-13)^2 = 0.170$, in good agreement with that expected.

One can expect considerable fluctuation between ADEV and MDEV stability plots for real data especially at longer averaging factors.

ANALYTICAL EXPRESSIONS AND ASYMPTOTICAL VALUE FOR R(n)
(Results Are Valid within Condition $2\pi f_c \tau_0 \gg 1$)

α	R(n)	$\lim_{n \rightarrow \infty} R(n)$
2	$\frac{1}{n}$	0
1	$\frac{1}{n^2} \left[n + \frac{1}{3 \ln(2\pi f_c \tau_0)} \times \sum_{k=1}^{n-1} (n-k) \left\{ 4 \ln \left(\frac{n^2}{k^2} - 1 \right) - \ln \left(\frac{4n^2}{k^2} - 1 \right) \right\} \right]$	0
0	$\frac{n^2 + 1}{2n^2}$	0.5
-1	$\frac{1}{n^2} \left[\frac{4n^2 - 3n + 1}{2} + \frac{1}{n^2 \ln^2} \times \sum_{k=1}^{n-1} (n-k) \times \left\{ \frac{n}{2} \left[(k+2n) \ln(k+2n) - (k-2n) \ln(2n-k) \right] + \frac{1}{2} (k+n)(k-2n) \ln(k+n) + \frac{1}{2} (k-n)(k+2n) \ln k-n + 3k^2 \ln k - k \left[(n+2k) \ln \left(k + \frac{n}{2} \right) - (n-2k) \ln \left(k - \frac{n}{2} \right) \right] \right\} \right]$	0.787
-2	$\frac{33}{40} + \frac{1}{8n^2} + \frac{1}{20n^4}$	0.825

Figure 16. Analytical Expressions for R(n) (From [4])

The original 1981 Allan and Barnes MVAR paper [5] contained an empirical expression for R(n)⁹, and this table from the 1984 Lesage and Ayi MVAR paper [4] contains analytical expressions for it¹⁰. Those results are superseded in part by those of Reference [1] as shown in Figures 9 and 10 and the discussion in its Section A.6. Additional expressions regarding ADEV and MDEV are shown in Figure 17.

⁸ One therefore cannot see the F FM dependence on system hardware bandwidth.

⁹ See the errata note #34 in [1].

¹⁰ See the correction for $\alpha = -1$ in Section A.6 of [1].

Noise type	$S_\varphi(f)$	$\sigma_y^2(\tau)$	Mod $\sigma_y^2(\tau)$	$\frac{\text{MVAR}}{\text{AVAR}}$	$\frac{\text{MVAR}}{\text{AVAR}}, \text{ dB}$
Large bump $B_b > 1/\tau$	b_b	$\frac{3 P_b}{4\pi^2 v_0^2} \tau^{-2}$	$\frac{5}{8\pi^4 (f_b^2 - B_b^2/4)} \frac{P_b}{v_0^2} \tau^{-4}$	1.1×10^{-58}	-49.5^{\S}
Narrow bump $B_b < 1/\tau$	$ f - f_b < \frac{B_b}{2}$ $P_b = b_b B_b$ $f_h > f_b + B_b/2$	$\frac{2}{\pi^2} \sin^4(\pi f_b \tau) \frac{P_b}{v_0^2} \tau^{-2}$	$\frac{2}{\pi^4 f_b^2} \sin^6(\pi f_b \tau) \frac{P_b}{v_0^2} \tau^{-4}$	-	-
Blue PN	$b_1 f^1$	$\frac{3 f_h^2 b_1}{8\pi^2 v_0^2} \tau^{-2}$	$\frac{9.643 + 10 \ln(\pi f_h \tau)}{16\pi^4} \frac{b_1}{v_0^2} \tau^{-4}$	$2.6 \times 10^{-5*}$	-45.9^*
White PN	b_0	$\frac{3 f_h b_0}{4\pi^2 v_0^2} \tau^{-2}$	$\frac{3 b_0}{8\pi^2 v_0^2} \tau^{-3}$	0.005^*	-23.0^*
Flicker PN	$b_{-1} f^{-1}$	$\frac{1.038 + 3 \ln(2\pi f_h \tau)}{4\pi^2} \frac{b_{-1}}{v_0^2} \tau^{-2}$	$\frac{3 \ln(256/27)}{8\pi^2} \frac{b_{-1}}{v_0^2} \tau^{-2}$	0.166^*	-7.8^*
White FN	$b_{-2} f^{-2}$	$\frac{1}{2} \frac{b_{-2}}{v_0^2} \tau^{-1}$	$\frac{1}{4} \frac{b_{-2}}{v_0^2} \tau^{-1}$	0.5	-3.0
Flicker FN	$b_{-3} f^{-3}$	$2 \ln(2) \frac{b_{-3}}{v_0^2}$	$\frac{27}{20} \ln(2) \frac{b_{-3}}{v_0^2}$	0.675	-1.7
Random Walk FN	$b_{-4} f^{-4}$	$\frac{2\pi^2 b_{-4}}{3 v_0^2} \tau$	$\frac{11\pi^2 b_{-4}}{20 v_0^2} \tau$	0.825	-0.8
Linear frequency drift \dot{y}	-	$\frac{1}{2} (\dot{y})^2 \tau^2$	$\frac{1}{2} (\dot{y})^2 \tau^2$	1	0

Table 1: AVAR and MVAR for several noise processes; these formulae hold for $f_h \tau \gg 1$ and $n \gg 1$. v_0 is the frequency of the optical carrier; f_h is the measurement bandwidth; the bump parameters: P_b, f_b, B_b and b_b are defined in Sec. II.D. The ratio MVAR/AVAR has been calculated for $f_h \tau = 100$ (*) and for $f_b \tau = 100$ and $f_b = B_b$ (§);

Figure 17. AVAR and MVAR Expressions (From [34])

In particular, see the expressions for White PN through RW FN. Note that the b_α terms are more commonly denoted as h_α .

Per [3] and [15], MDEV is independent of the averaging factor, n , for n greater than some minimum value that depends on the noise type(s).

• Sampling Functions

The sampling functions associated with ADEV and MDEV calculations that determine their spectral properties (i.e., frequency domain filtration) are shown in Figures 18 and 19 respectively.

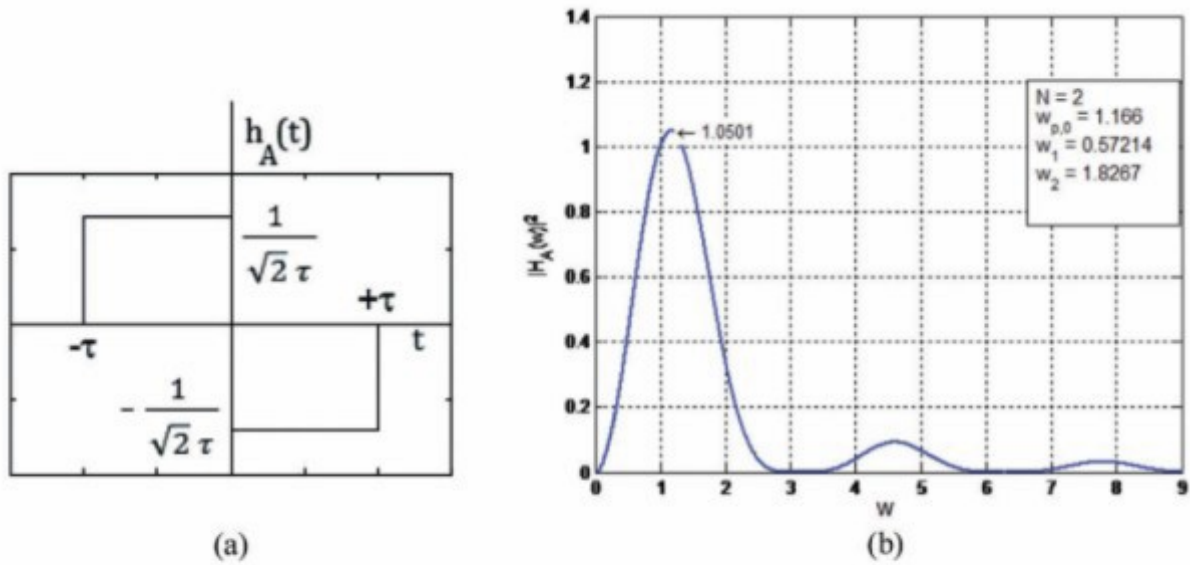


Fig. 13. – Impulse response (a) and power frequency response (b) of the AVAR algorithm.

Figure 18. AVAR Sampling Function and Frequency Response (From [36])

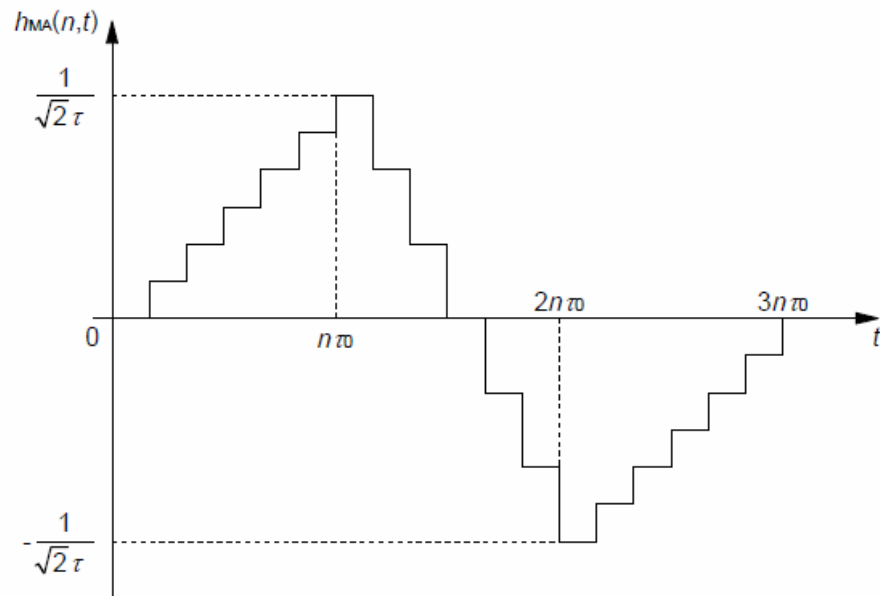


Fig. 1: Impulse response $h_{MA}(n,t)$ of the filter associated to the definition of Modified Allan Variance for $n=6$.

Figure 19. Impulse Response of the MVAR Sampling Function (for $n=6$) (From [8])

The frequency response of AVAR, shown in Figure 20, determined by the Fourier transform of its sampling function, looks like a half-octave-wide bandpass filter. The peak in the response is at $f = 0.5/\tau_0$, where f is a Fourier component of fractional frequency deviation $y(t)$ and τ_0 is the basic sampling time of the frequency data. Because there is considerable energy in the sidelobes (the 2nd one is only about -10 dB) one should not restrict the measurement bandwidth to less than about x2 the peak response, or about $(\tau_0)^{-1}$.

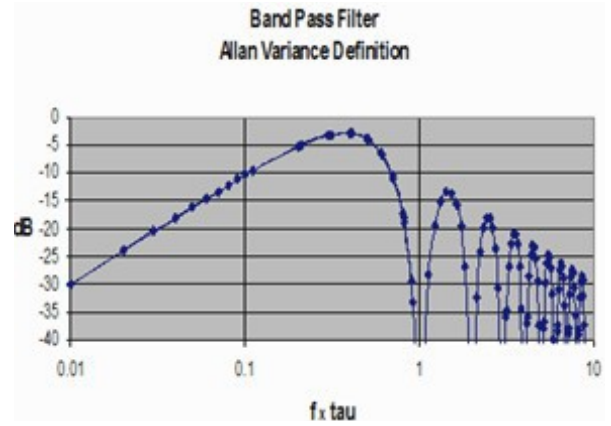


Figure 20 AVAR Filter Response (From [23])

• Transfer Functions

AVAR and MVAR transfer functions are shown in Figures 21 and 22.

The ADEV has a frequency domain transfer function of:

$$|H(f)|^2 = 2 \cdot \frac{\sin^4(\pi \cdot \tau \cdot f)}{(\pi \cdot \tau \cdot f)^2}, \quad (10)$$

where $\tau = n \cdot \tau_0$.

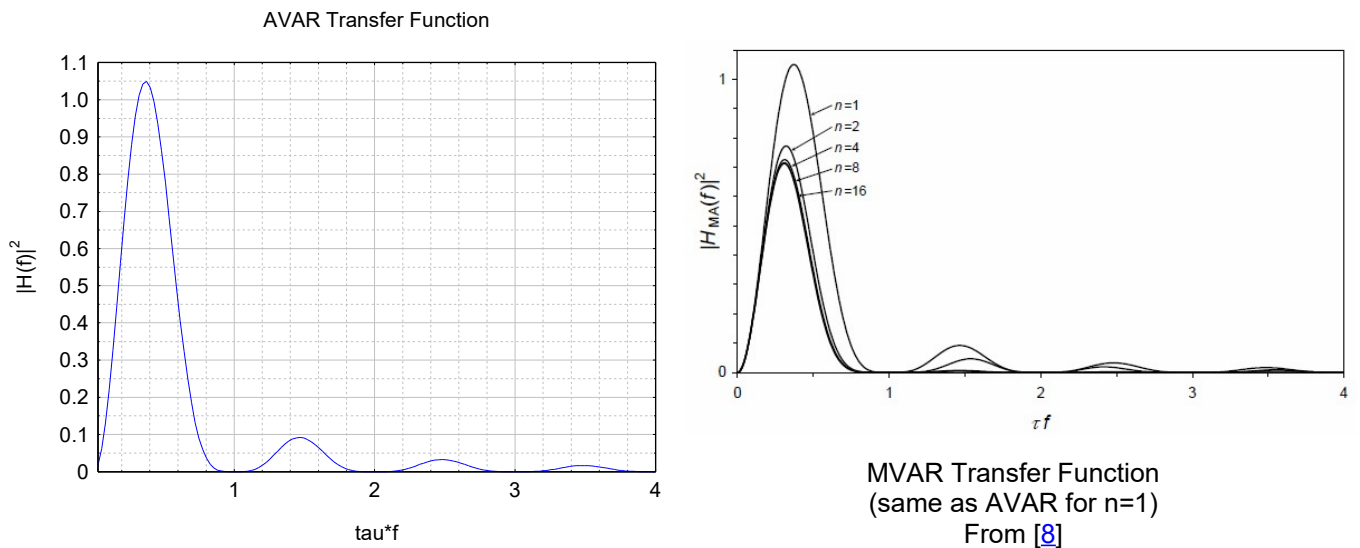


Figure 21. AVAR and MVAR Transfer Functions

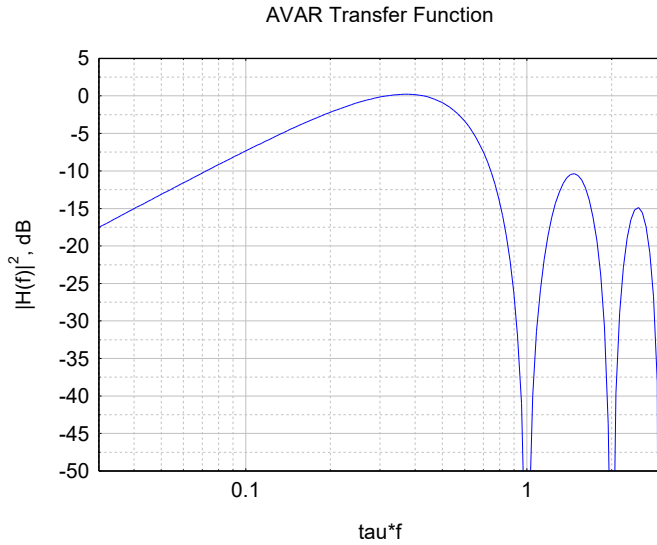


Figure 22. AVAR Transfer Function, dB

The MDEV has a frequency domain transfer function of:

$$|H(f)|^2 = 2 \cdot \frac{\sin^6(\pi \cdot f \cdot n \cdot \tau_0)}{(\pi \cdot f \cdot n^2 \cdot \tau_0)^2 \cdot \sin^2(\pi \cdot f \cdot \tau_0)} \quad (11)$$

The fairly narrow AVAR and MVAR spectral responses allow them to serve as a means of spectral analysis, enabling them to resolve periodic frequency fluctuations (see Figure 12 bottom left, and Sections 11.4 and 11.5 of [14]). AVAR/MVAR analyses are typically run over a range of octave-spaced averaging times, and their composite spectral response is quasi-rectangular as shown in Figures 23 and 24 [9], [16].

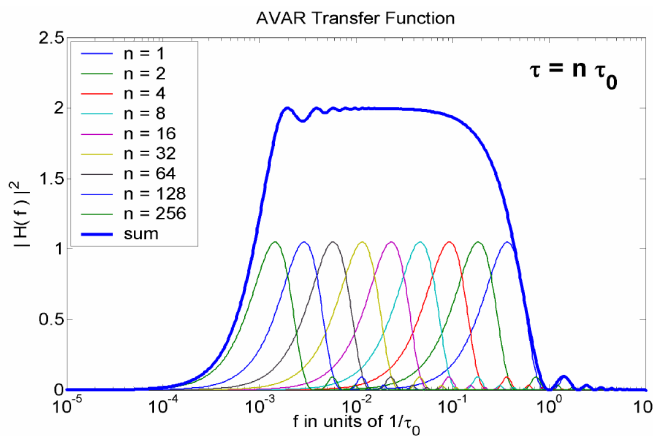


Figure 23. AVAR Octave-Spaced Composite Transfer Function

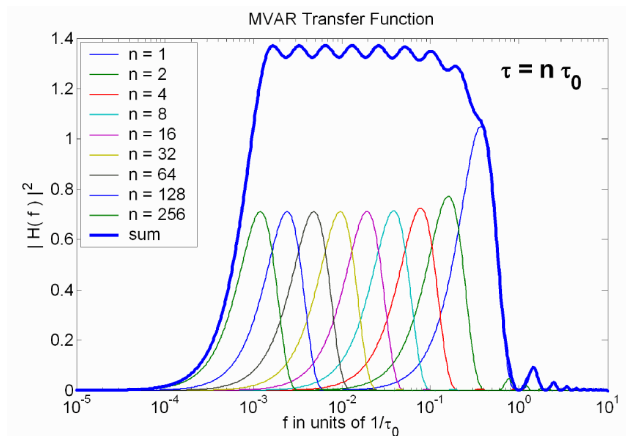


Figure 24. MVAR Octave-Spaced Composite Transfer Function

- **Frequency Domain Expressions**

ADEV and MDEV can be expressed in the frequency domain in terms of the spectral density of the fractional frequency fluctuations, $S_y(f)$ as follows (see [2]):

$$\sigma_y^2(\tau) = 2 \cdot \int_0^{f_h} S_y(f) \frac{\sin^4(\pi f \tau)}{(\pi f \tau)^2} df, \quad (12)$$

where $\tau = n \cdot \tau_0$, and

$$Mod \sigma_y^2(n \tau_0) = 2 \cdot \int_0^{f_h} S_y(f) \frac{\sin^6(\pi f n \tau_0)}{(\pi f n^2 \tau_0)^2 \cdot \sin^2(\pi f \tau_0)} df. \quad (13)$$

These integrals show the additional filtration provided by MVAR. They can be used in numerical calculations to determine ADEV and MDEV from frequency domain (spectral) measurements (see [3]). The upper integration limits are set by the system bandwidth, f_h . These expressions are thus the basis for time-frequency domain conversions.

- **Domain Conversions**

Conversions between time (e.g., ADEV, MDEV) and frequency domain (e.g., $S_y(f)$, $\mathcal{L}(f)$) stability measurers are possible via these integrals either by numerical integration [31] or power law noise relationships (see Section 7 of [14] or Annex 1, Section 4 of [19]). The Stable32 Domain function supports those conversions.

- **ADEV and MDEV Confidence Limits**

ADEV and MDEV results should include an indication of their confidence limits, e.g., error bars on a stability plot. Setting those bounds (the variance of a variance) involves Chi-squared statistical methodology, which depend on the variance type (AVAR or MVAR), dominant power-law noise type (W PM through RW FM), the number of analysis data points, and the desired confidence factor (e.g., 1-sigma, 68%). Doing so requires a means for determining the number of Chi-squared equivalent degrees of freedom (edf) for the particular variance type, noise type, and number of data points. That is basically a three-step process, estimating the power law noise type and then the df, and finally setting the confidence limits.

Several methods are available for power-law noise identification (see Section 5.5 of [14]). A particularly effective way is via the lag 1 autocorrelation function, r_1 , applied to the phase or frequency data (see [31]).

Sample variances are distributed according to the expression:

$$\chi^2 = \frac{edf \cdot s^2}{\sigma^2}, \quad (14)$$

where χ^2 is the Chi-square, s^2 is the sample variance, σ^2 is the true variance, and edf is the # of degrees of freedom (not necessarily an integer). Double-sided confidence limits are then set with:

$$\sigma^2_{\min} = s^2 \cdot \frac{edf}{\chi^2(p, edf)} \quad \text{and} \quad \sigma^2_{\max} = s^2 \cdot \frac{edf}{\chi^2(1-p, edf)} \quad (15)$$

where p is the one-half of the desired confidence factor. Single-sided confidence limits can be set with the 2nd expression only and $2p$ ¹¹.

• Frequency Stability Measurements

A canonical frequency measurement is made with a frequency counter having adequate resolution, zero dead-time, and an accurate and stable reference. A canonical phase measurement would be made with a time interval counter with those attributes. In practice, a variety of devices and systems have been devised for those purposes, with phase measurements generally being preferred. The resulting data is normally unprocessed and unfiltered (although the measuring system may impose a bandwidth limit), and is suitable for whatever analysis may follow. However it is possible that the system may perform some sort of phase averaging as a means for noise reduction, and, in that case, the resulting data may resemble an MVAR process¹². Increasingly, such processing may be hidden in internal firmware¹³.

• Dead Time

Dead time can be a problem when analyzing discontinuous frequency measurements when the spacing between them is a significant fraction of the measurement interval (this issue does not apply to phase measurements) [27]. The extent of the effect of dead time on an ADEV analysis also depends on the dominant power law noise type, with the least effect for white FM noise ($\alpha=0$) and the most effect when α most differs from 0 (white PM and random walk FM noise). Dead time can have a significant effect on the ADEV results.

Dead time between measurements is quite common in frequency measurements made with an ordinary frequency counter because of the delay caused by the counter between successive measurements. Dead time can also occur as the result of a deliberate wait between measurements (e.g. one $\tau = 100$ second measurement made once per hour). Dead time that occurs at the end of a measurement can be corrected for in an Allan deviation determination by using the Barnes B2 bias function [28], the ratio of the 2-sample variance with dead time ratio $r = T/\tau$ to the 2-sample variance without dead time. Otherwise, without this correction, one can only determine the average frequency and its drift. When such data are

¹¹ The Stable32 Sigma function can serve as an example for setting ADEV/MDEV error bars. A set of the desired power-law noise can be generated with the Noise function, and single or double-sided confidence limits can be established at a certain confidence factor. The corresponding edf and χ^2 parameters are shown.

¹² A classical or so-called Π counter (conventional, reciprocating or interpolating) makes a frequency measurement averaged over the measurement interval, equivalent to two phase samples at the beginning and end, a Δ counter makes multiple phase measurements at overlapping samples over the measurement interval, and a Ω counter uses a linear regression applied to multiple phase samples. The Greek letter names resemble the shapes of their respective phase sampling functions. They have Allan (AVAR), Modified (MVAR) and Quadratic (QVAR) variance responses at their basic measurement intervals.

¹³ Firmware for a DMTD clock measuring system developed by the author had optional phase averaging that displayed this behavior: MDEV response at τ_0 , mixed MDEV/ADEV response at small averaging factors, and ADEV response when the data were averaged to a longer tau. The noise floor was lowered and the short-term residual noise type was changed. This can be quite confusing, and one cannot measure ADEV at no/little averaging. But phase averaging does reduce a counter's internal W PM noise for ordinary average frequency measurements.

used to form frequency averages at longer tau, it is necessary to also use the B3 bias function [29], the ratio of the variance with distributed dead time to the variance with all the dead time at the end. Those bias corrections are made using the product of B2 and B3. The power law noise type must be known in order to calculate these bias functions. Simulated periodically sampled frequency data with distributed dead time for various power law noise processes shows significant bias without, and good agreement with, the B2 and B3 bias function corrections, as shown in Figures 25 and 26. These dead time corrections apply only to the ADEV.

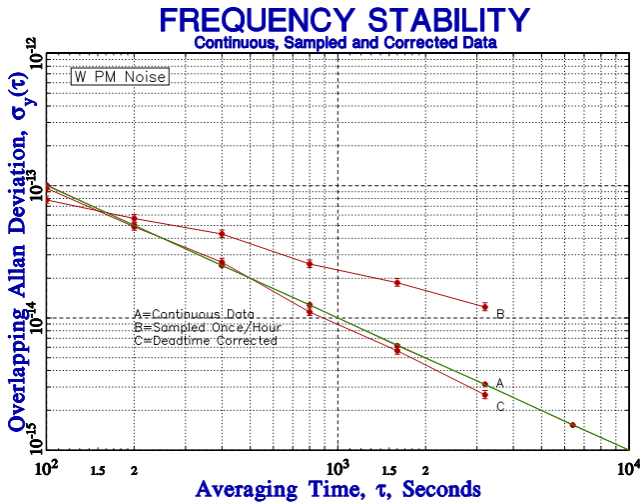


Figure 25. Deadtime correction for W PM noise

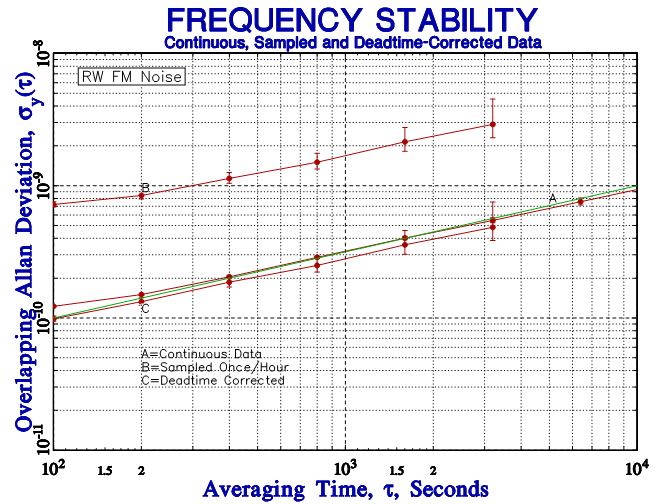


Figure 26. Deadtime correction for RW FM noise

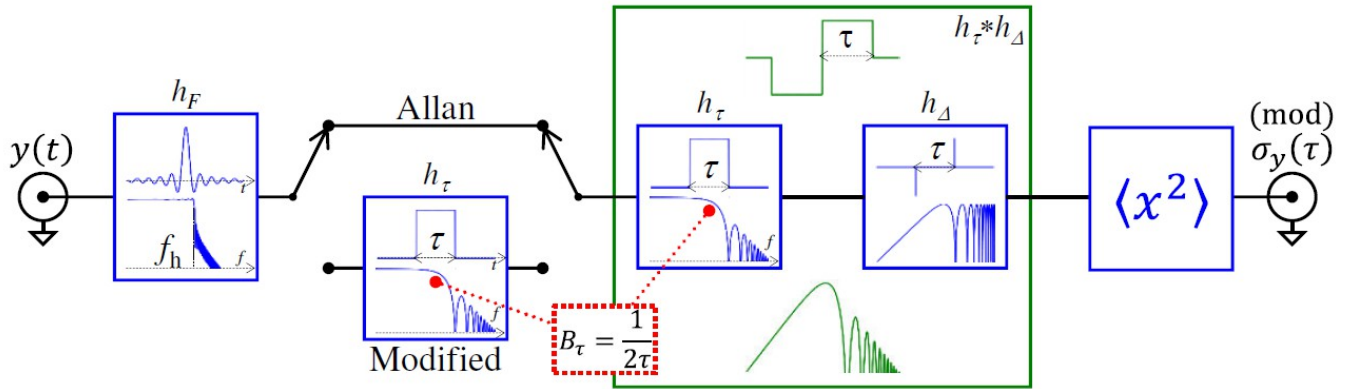
Frequency stability plots with large measurement dead time ($r = T/\tau = 36$) for W PM and RW FM noise. Simulated data sampled for $\tau = 100$ seconds once per hour for 10 days. Nominal 1×10^{-11} stability at $\tau = 100$ seconds shown by green lines. Plots show stability of simulated data sets for Continuous, Sampled and Dead Time-Corrected data.

• ADEV and MDEV Measurements

Phase or frequency measurements to support an ADEV or MDEV analysis can be made with a variety of instruments including frequency or time interval counters, dual mixer time difference (DMTD) systems, and RF sampling techniques [21]. These instruments produce streams of phase or frequency data, preferably the former, with timetags, suitable for an ADEV or MDEV analysis using either $x(t)$ phase in seconds or $y(t)$ dimensionless fractional frequency [22]. Be aware that some counters (so-called lambda Λ counters that have a triangular weighting function by using multiple overlapping phase samples) use internal phase averaging for noise reduction that distorts subsequent ADEV analysis¹⁴ [24]. An ADEV measurement is highly dependent on the system bandwidth for the case of white PM noise, less so for flicker PM noise. In the case of flicker PM noise, spectral aliasing can produce a spurious white PM noise component, but the ADEV results will be correct [23].

¹⁴ A frequency counter measures the input frequency averaged over a time τ_0 versus the reference clock. Higher resolution can be obtained by interpolation. Lower white PM noise can be obtained by averaging multiple overlapped measurements. But if such data is analyzed by an ADEV estimator, the result resembles that for a MDEV analysis. However if the data are averaged sufficiently to a longer tau, one obtains the expected ADEV response. This behavior can lead to misinterpretation.

A block diagram showing the ADEV or MDEV measurement process is shown in Figure 27. The source frequency fluctuations $y(t)$ enter at the left and the ADEV or MDEV results are obtained at the right. The source hardware noise bandwidth, f_h , filter can be either abrupt or tapered. An additional moving average filter with a radian bandwidth $(2\tau)^{-1}$ is included for MDEV. The green block represents the ADEV sampling function which introduces both lowpass and highpass filtration, the former also having a bandwidth of $(2\tau)^{-1}$. The last block is the statistical expectation operator.



Functional block diagram of the AVAR and of the MVAR. highlights the role of the measurement bandwidth f_h represented by the first block h_F (both impulse response and transfer function are shown); the switches allow selection between MVAR and AVAR, by enabling/disabling the additional moving average filter h_τ . Both h_F and h_τ are low-pass filters that reject fast noise, but the MVAR additional h_τ is less selective and changes its bandwidth with τ . The green block represents the well-known AVAR equivalent filter, i.e. the average h_τ over a time τ and the difference h_Δ between adjacent samples divided by $\sqrt{2}$; the last block evaluates the mean power.

Figure 27. ADEV and MDEV Processing Block Diagram (From [34])

The bandwidth considerations for an ADEV or MDEV analysis can be divided into three categories: that of the source hardware, the measurement sampling process, and the analysis software. They apply mainly to white and flicker PM noise such as exists as a dominant mechanism in certain spectral regions of crystal oscillators (e.g., the oscillator active device above the resonator half-bandwidth, and additive noise from the output amplifier), and active H-masers (e.g., receiver thermal noise). PM noise can also be contributed by the measurement system instrumentation (e.g., wideband counter input circuits) and data quantization.

Besides the source itself, the fixed hardware bandwidth f_h also depends on such factors as crystal filters and PLL loops. It is generally much wider than the measuring system Nyquist frequency, one-half of the reciprocal of the sampling rate, τ_0 . If not, the system bandwidth will effect the measurement and should be noted.

The measurement sampling process is thus usually subject to aliasing, and has an effect on the spectral properties of the data, but it does not affect the total noise power or the variance [23]. In the case of W PM noise, the sampled noise remains the same spectral type. In the case of F PM, some of the noise power becomes W PM, with the same total variance.

The analysis software bandwidth is even less, one-half of the reciprocal of the analysis τ for ADEV and is further narrowed by the averaging factor by the MDEV phase averaging.

• ADEV and MDEV Computation

ADEV and MDEV computation is practically instantaneous when performed using phase data with compiled code on modern computers, even for very large (e.g., 10^6 point) data sets [26]. Outliers must be removed before proceeding with an analysis. It is generally best to remove any deterministic frequency drift before analyzing the stochastic noise. Frequency offset is usually not a problem, even with regard to the dynamic range of high stability phase data having a large frequency offset (slope). A sigma-tau run is usually done at octave or sub-decade (e.g., 4 points/decade) increments, but it is perfectly practical to show every possible averaging factor (“all tau”) or a sufficient subset of them (“many tau”), say 500, to visually fill a plot. Gaps in phase or frequency data may either be skipped if a value contributes to an analysis point (and gradually averaged away), or filled with interpolated values (the latter may lead to strange results if overdone) [27]. Error bars are usually shown, particularly for octave or sub-decade increments, and the dominant noise type and edf must be determined point-by-point to properly set them (see Section 5.4.1 of [14]). The number of stability points with reasonable confidence produced by an octave run for N data points is approximately $\log_2(N/4)$. It is common to fit a power law noise line to all or a portion of a sigma-tau plot. Corrections for dead time and assumed identical reference noise may be wanted. The plot may be accompanied by a table of the numeric values, and various labels and annotations may be supported.

• Sigma-Tau Plot Fluctuations

The points on a sigma-tau plot (ADEV, MDEV, etc.), with octave, decade, “all tau”, or “many tau” spacing, are seldom a straight line following a power law but rather exhibit various fluctuations. Some of those are simply statistical scatter (the variance of a variance), but others seem to have distinct patterns, some of which represent information about the device under test or its environment, and others that are artifacts of either the measurement or analysis process.

An ADEV analysis is a form of spectral analysis whose properties are determined by the transfer function of its sampling/estimation process. This can offer valuable insight into the behavior of the device under test, particularly its environmental sensitivity. Examples are periodic fluctuations caused by vibration, temperature cycling, power line interference, power supply ripple, and the like. The ADEV plot will show nulls at the period of the interfering signal, peaks at its half-periods, maxima representing the peak interference amplitude, and minima representing the undisturbed stability (see Section 11.5 of [14]). If the interference frequency is higher than one-half the measurement sampling rate, one will experience aliasing and slow beat note fluctuations.

An ADEV plot will generally show a “collapse” at long averaging factors, those beyond which there are sufficient analysis points for good confidence. Those points should be ignored, and, if needed, consideration should be given to using an enhanced statistic like the Total variance or $\text{Th}\varrho_1$. The ADEV drop off is an expected property of the Chi-squared distribution that governs statistical variances.

More confusing are other quasi-periodic fluctuations [30]. Those effects can result from interference between the ADEV sampling response and long-period divergent noise, because the number of Chi-squared degrees of freedom is small, by data turn-on “ringing”, or because of leakage from wideband PM noise. Those effects are independent from issues of aliasing, and the solution can again be to use the more capable Total or $\text{Th}\varrho_1$ estimators.

• Conclusions

The following are a few of general rules for characterizing the stability of a frequency or timing source:

1. Separate the deterministic and stochastic aspects of device behavior. For either a frequency, timing, or RF source, remove its frequency offset and aging, and its environmental sensitivity and drift, before analyzing its noise per item (2).
2. Specify or analyze the device noise in the domain and with a method that closely resembles the requirement. Use the ADEV for a frequency source. Use the MDEV/TDEV for a timing source. Use a spectral density for an RF source. RMS jitter is an alternative for a clock, RMS phase noise or residual FM for an oscillator.
3. The measuring system often resembles the application (e.g., a time interval counter for a timing system, a spectrum analyzer for an RF source). Heterodyne techniques are a common way to enhance measuring system resolution. Zero dead time phase measurements are preferred, even for long-term stability runs. Reference stability is critical. Coherent inputs are a common way to assess measuring system noise floor. One should always have a good understanding about what is inside a “black box” measuring instrument’s hardware and firmware or analysis software.

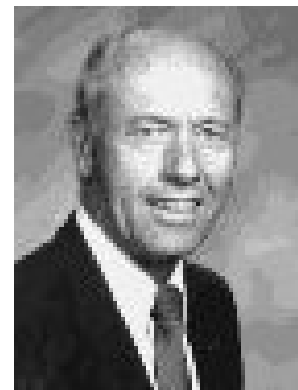
We emphasized the time domain analysis methods herein. ADEV is generally the frequency stability measure of choice, with MDEV as a PM noise diagnostic, while TDEV is generally the best time stability measure. Most analysts are content to simply use the Allan deviation to characterize frequency source stability. Some others will use the Modified Allan deviation to resolve white/flicker PM noise ambiguity or implicitly in a time deviation determination. Stability analysis software will hide the details for most users. Nevertheless, it is important that all such analysts have a good understanding of the underlying statistical principles and ready access to reference material when deeper insight is needed.

• Acknowledgments

The field of modern frequency stability analysis was initiated by J.A. Barnes and D.W. Allan at the U.S National Bureau of Standards (NBS, now the National Institute of Standards and Technology, NIST)¹⁵. I acknowledge their work and that of the others who subsequently developed additional frequency stability measures and provided insights into frequency stability analysis, some of which are referenced and excerpted herein.



Dr. J.A. “Jim” Barnes
1933-2002



Dr. D.W. “Dave” Allan
1936-

¹⁵ David Allan’s 1965 Master’s thesis gave birth to the Allan variance under the guidance of Jim Barnes. Later, in 1981, they developed the Modified Allan variance and, with colleagues at NBS, the Time variance, all three of which became international standards. See the special [2016 50th anniversary commemorative issue of the IEEE UFFC Transactions](#) and References [5], [7], [17], [25] and [26].

• References

1. D.B. Sullivan, D. W. Allan, D. A. Howe, and F. L. Walls, Eds., NIST Technical Note 1337, [*Characterization of Clocks and Oscillators*](#), February 1990. This compilation of papers includes references [10], [4], [5] and [35].
2. J. Rutman and F.L.Walls, “[Characterization of Frequency Stability in Precision Frequency Sources](#)”, *Proceedings of the IEEE*, Vol. 79, No. 6, pp. 952-960, June 1991.
3. F.L. Walls, et al., [Time Domain Frequency Stability Calculated From the Frequency Domain Description: Use of the SIGINT Software Package to Calculate Time Domain Frequency Stability from the Frequency Domain](#), NISTIR 89-3916 Revised, September 1991.
4. P. Lesage and T. Ayi, “[Characterization of Frequency Stability: Analysis of the Modified Allan Variance and Properties of Its Estimate](#)”, *IEEE Transactions on Instrumentation and Measurement*, Vol. IM-33, No. 4, December 1984.
5. D.W. Allan and J.A. Barnes, “[A Modified Allan Variance with Increased Oscillator Characterization Ability](#)”, *Proceedings of the 35th Annual Frequency Control Symposium*, pp. 470-474, May 1981.
6. J.A. Davis, “[Introduction to atomic clocks and statistics for time and frequency](#)”, CLONETS Clock Network Services, February 2019.
7. D.W. Allan, “[The Statistics of Atomic Frequency Standards](#)”, *Proceeding of the IEEE*, Vol. 54, No. 2, pp. 221-230, February 1966. This is the “classic” reference introducing the 2-sample variance (later known as the Allan variance).
8. S. Bregni and L. Primerano, “[Using the Modified Allan Variance for Accurate Estimation of the Hurst Parameter of Long-Range Dependent Traffic](#)”, *IEEE Transactions on Information Theory*, Submitted February 2005.
9. D.W. Allan, “[Conversion of Frequency Stability Measurers from the Time-domain to the Frequency-domain, vice-versa and Power-law Spectral Densities](#)”, www.allanstime.com, January 2012.
10. J. A. Barnes *et al.*, “[Characterization of Frequency Stability](#),” *IEEE Transactions on Instrumentation and Measurements*, Vol. 20, No. 2, pp. 105–120, May 1971.
11. J. Rutman, “[Characterization of Phase and Frequency Instabilities in Precision Frequency Sources: Fifteen Years of Progress](#),” *Proceedings of the IEEE*, Vol. 66, No. 9, pp. 1048–1075, September 1978.
12. S. Bregni, “[Clock Stability Characterization and Measurement in Telecommunications](#),” *IEEE Transactions on Instrumentation and Measurements*, Vol. 46, No. 6, pp. 1284–1294, December 1997.
13. S. Bregni, “Chapter 5—Characterization and Modeling of Clocks,” in [Synchronization of Digital Telecommunications Networks](#), Wiley, 2002, pp. 203–281.
14. W. J. Riley, [Handbook of Frequency Stability Analysis](#), National Institute of Standards and Technology, Special Publication 1065, July 2008.
15. L. G. Bernier, “[Theoretical Analysis of the Modified Allan Variance](#),” in *Proceedings of the 41st Annual Frequency Control Symposium*, May 1987, pp. 116–121.
16. D.W. Allan, M. A. Weiss, and J. L. Jespersen, “[A Frequency-Domain View of Time-domain Characterization of Clocks and Time and Frequency Distribution Systems](#),” in *Proceedings of the 45th IEEE Annual Frequency Control Symposium*, May 1991, pp. 667–678.
17. D. W. Allan, D. D. Davis, J. Levine, M. A. Weiss, N. Hironaka, and D. Okayama, “[New Inexpensive Frequency Calibration Service from NIST](#),” *Proceedings of the 44th Annual IEEE Frequency Control Symposium*, June 1990, pp. 107–116.
18. C. A. Greenhall, “[The Third-Difference Approach to Modified Allan Variance](#),” *IEEE Transactions on Instrumentation and Measurements*, Vol. 46, No. 3, pp. 696–703, June 1997.
19. ITU Recommendation TF.538-4, [Measures for Random Instabilities in Frequency and Time \(Phase\)](#), International Telecommunication Union, August 2017.

20. IEEE Std. 1139-2008, [IEEE Standard Definitions of Physical Quantities for Fundamental Frequency and Time Metrology--Random Instabilities](#), February 2009.
21. W.J. Riley, "[Time and Frequency Measurements](#)", Hamilton Technical Services web site, April 2019.
22. W.J. Riley, "[The Strange Case of a Pseudo Flicker Floor](#)", Hamilton Technical Services web site, May 2019.
23. W.J. Riley, "[The Bandwidth Dependence of Time Domain Frequency Stability Measurements](#)", Hamilton Technical Services web site, May 2020.
24. E. Rubiola, "[On the Measurement of Frequency and of its Sample Variance with High-Resolution Counters](#)", arXiv:physics/0411227v2, *Review of Scientific Instruments*, Vol. 76, Article No. 054703, May 2005.
25. Wikipedia, "[Allan Variance](#)".
26. W.J. Riley, "The [Evolution of Frequency Stability Analysis Software](#)", Hamilton Technical Services web site, July 2014.
27. W.J. Riley, "[Gaps, Outliers, Dead Time, and Uneven Spacing in Frequency Stability Data](#)", Hamilton Technical Services web site, October 2006.
28. J.A. Barnes, "Tables of Bias Functions, B1 and B2, for Variances Based on Finite Samples of Processes with Power Law Spectral Densities", *NBS Technical Note 375*, January 1969.
29. J.A. Barnes and D.A. Allan, "[Variances Based on Data with Dead Time Between the Measurements](#)", *NIST Technical Note 1318*, 1990.
30. D.A. Howe, "[Interpreting Oscillatory Frequency Stability Plots](#)" *Proceedings of the 2002 IEEE International Frequency Control Symposium*, pp. 725-732, May 2002.
31. W.J. Riley and C.A. Greenhall, "[Power Law Noise Identification Using the Lag 1 Auto-correlation](#)," *Proceedings of the 18th European Frequency and Time Forum*, April 2004.
32. N.J. Kasdin and T.Walter, "[Discrete Simulation of Power Law Noise](#)", *1992 IEEE Frequency Control Symposium* , pp. 274-283, May 1992.
33. W.J. Riley, "[The Statistics of Time Transfer](#)", Tutorial at the 2016 ION Precise Time and Time Interval (PTTI) Meeting, January 2016.
34. C.E. Calosso, C. Clivati, and S. Micalizio, "Avoiding Aliasing in Allan Variance: an Application to Fiber Link Data Analysis", <https://arxiv.org/pdf/1512.03810>.
35. S.R. Stein, "[Frequency and Time – Their Measurement and Characterization](#)", Chapter 12, pp. 191-416, *Precision Frequency Control*, Vol. 2, Edited by E.A Gerber and A. Ballato, Academic Press, New York, 1985, ISBN 0-12-280602-6.
36. E. Bava, "[Frequency Instability: Characterization of Quasi-Periodic Signals](#)," *Proceedings of the International School of Physics "Enrico Fermi" Course 185, "Metrology and Physical Constants"*, 2013.

Appendix 1

Non-Convergence of the Standard Variance for Flicker and Random Walk FM Noise

This figure from Reference [35] shown the non-convergence of the standard variance, denoted by $\sigma^2(N, \tau)$, for flicker FM ($\alpha=-1$) and random walk FM ($\alpha=-2$) power law noise (see also Figure 1 of Reference [14]). For those divergent noise types, the standard variance depends on the number of samples used for its estimation while the Allan (and related) statistics do not. This was the basis for the development of the Allan variance, and was an important milestone in the analysis of frequency stability.

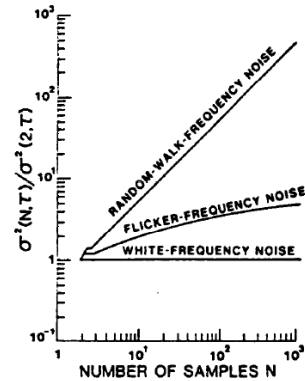


FIG. 12-4 N -sample variance versus Allan variance. The two-sample variance converges for the important types of noise observed in frequency standards but the ratio of the traditional variance to the two-sample variance is an increasing function of sample size for flicker frequency noise and random-walk frequency noise.